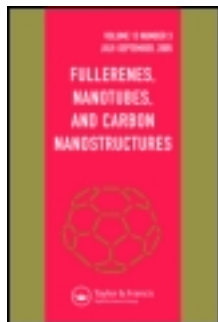


This article was downloaded by: [UNAM Ciudad Universitaria]
On: 18 June 2012, At: 11:18
Publisher: Taylor & Francis
Informa Ltd Registered in England and Wales Registered Number: 1072954
Registered office: Mortimer House, 37-41 Mortimer Street, London W1T 3JH,
UK



Fullerene Science and Technology

Publication details, including instructions for authors and subscription information:

<http://www.tandfonline.com/loi/lfnn19>

The Role of Boron Nitride in Graphite Plasma Arcs

M. Terrones^a, W. K. Hsu^a, S. Ramos^b, R. Castillo^b
& H. Terrenes^b

^a School of Chemistry, Physics and Environmental Science, University of Sussex, Brighton, BN1 9QJ, U. K.

^b Instituto de Fisica, UNAM, Apartado Postal 20-364 01000, México, D. F.

Available online: 23 Apr 2008

To cite this article: M. Terrones, W. K. Hsu, S. Ramos, R. Castillo & H. Terrenes (1998): The Role of Boron Nitride in Graphite Plasma Arcs, *Fullerene Science and Technology*, 6:5, 787-800

To link to this article: <http://dx.doi.org/10.1080/10641229809350240>

PLEASE SCROLL DOWN FOR ARTICLE

Full terms and conditions of use: <http://www.tandfonline.com/page/terms-and-conditions>

This article may be used for research, teaching, and private study purposes. Any substantial or systematic reproduction, redistribution, reselling, loan, sub-licensing, systematic supply, or distribution in any form to anyone is expressly forbidden.

The publisher does not give any warranty express or implied or make any representation that the contents will be complete or accurate or up to date. The accuracy of any instructions, formulae, and drug doses should be

independently verified with primary sources. The publisher shall not be liable for any loss, actions, claims, proceedings, demand, or costs or damages whatsoever or howsoever caused arising directly or indirectly in connection with or arising out of the use of this material.

The role of boron nitride in graphite plasma arcs

M. Terrones ^a, W. K. Hsu ^a, S. Ramos ^b, R. Castillo ^b, H. Terrones ^b

^a *School of Chemistry, Physics and Environmental Science,
University of Sussex, Brighton BN1 9QJ, U. K.*

^b *Instituto de Física, UNAM, Apartado Postal 20-364
01000 México, D. F.*

Novel graphitic nanostructures (e.g. nanotubes, graphitic onions, polyhedral particles, hemitoroidal nanotube caps and branched nanotubes) are produced by arcing graphite electrodes, containing hexagonal-BN, in inert atmospheres. The introduction of BN or B inside the graphite anode generates long ($\leq 20\mu\text{m}$) and well graphitised carbon nanotubes exhibiting boron at their tips. High Resolution Electron Microscopy (HRTEM), Scanning Electron Microscopy (SEM), Electron Energy Loss Spectroscopy (EELS) and X-ray powder diffraction studies reveal the production of B_4C crystals, in addition to little amounts of BC_3 nanotubes. Mass spectrometry (MS) studies over the generated soots indicate high yields of large fullerenes (e.g. C_{70} , C_{76} , and C_{84}) and thermo-Gravimetric analysis (TGA) of the nanostructures show high oxidation resistance.

1. INTRODUCTION

Following the discovery of fullerenes¹ and their bulk production², novel graphitic structures (e.g. carbon nanotubes^{3,4}, graphitic onions⁵ or giant concentric fullerenes⁶) were observed and/or recognised by HRTEM from the deposits generated on the cathode during arc-discharge between two graphite electrodes in inert atmospheres^{2,3,4,6}. Lately, new methods for the production of fullerenes and graphitic nano-structures have been developed involving pyrolysis⁷⁻¹⁰ and flame combustion¹¹ of hydrocarbons, laser irradiations over graphite^{12,13} and electrolysis

of graphite electrodes in molten ionic salts^{14,15}. Moreover, it proved possible to encapsulate metal oxides¹⁶, ferromagnetic materials¹⁷ and superconducting nanocarbitides¹⁸⁻²⁰ inside nanotubes and graphitic nanoparticles with potential applications in magnetic data storage, magnetic toners, inks for xerography, superconducting nano-circuits in electronics, *etc.* Additionally, pyrolytic methods have brought the possibility to generate helix-shaped nanotubes^{21,22}, hemitoroidal nanotubes^{10,23,24} and bent nanotubes^{24,25}, in which, the influence of heptagons and pentagons in the predominantly hexagonal network seems to be responsible for negative curvature^{22,26,27}.

Other layered materials, such as MoS₂²⁸, WS₂²⁹, BC₂N^{30,31}, BC₃³⁰, BCN³² and BN³³⁻³⁵, have recently been shown to form closed concentric shells (onions) and nanotubes. The production of these novel graphite-like nanostructures offer potential application in material sciences and nano-scale engineering due to their conducting properties and oxidation resistance.

In this paper we discuss various structural effects of nanomaterials generated using graphite plasma arcs in presence of BN or B. The by-products contain hemitoroidal nanotube caps and negatively curved graphite structures among nanotubes, nanofibres and polyhedral particles. Large quantities of well graphitised *long* carbon nanotubes ($\leq 20\mu\text{m}$) are obtained. BC₃ nanotubules, arranged in hexagonal networks similar to those in graphite, have also been produced. Mass spectrometry studies show that higher yields of large fullerenes are obtained when BN/B-graphite mixtures are arced. HRTEM, SEM, EELS, X-ray powder diffraction, MS and TGA studies of these structures are presented.

2. EXPERIMENTAL

Samples were prepared using an arc-discharge DC generator employed for fullerene production. Anode graphite rods (6 mm diameter) were drilled (4mm. OD, 3 cm length) and B, B₂O₃, BN powders (99.9% Aldrich Co.) introduced. In some cases, graphite cement (AREMCO PRODUCTS INC.) was mixed with such powders and inserted into drilled graphite anodes followed by heat treatment (3 hours at 300 °C). The cathodes used consisted of graphite rods with different diameters (6 mm and 200 mm.).

Before arcing operations, the chamber was evacuated and purged with nitrogen or helium (air products 99.9%) twice. The chamber was finally set

between 200-500 Torr of gas pressure. Our operation conditions varied from 25V, 80 Amp to 40V, 150 Amp. A gap between electrodes was maintained to *ca.* 1 mm. The resulting inner core cathode deposits were analysed by X-ray powder diffraction (SIEMENS D-5000, Cu-K α radiation).

HRTEM studies were carried out using: JEM4000 at 400 keV and a Hitachi 7100 at 125 kV. A few mg from the inner core (cathode) deposit were sonicated in acetone for 5 min and then placed on Cu perforated carbon grids for HRTEM observations. SEM images were obtained using a Leo 5420 at 20 keV.

TGA analysis from the inner core cathode deposits were recorded in a Perkin-Elmer 7 Thermogravimetric Analyzer. For all MS studies (VG Autospec, electron impact 70 eV), soots scraped from the reactor chamber walls were washed in acetone and dissolved in CS₂.

3. RESULTS AND DISCUSSION

3.1 Electron Microscopy Studies

TEM and HRTEM images from the inner core cathode deposits exhibit long carbon nanotubes ($\leq 20 \mu\text{m}$.) possessing small amounts of polyhedral particles (nanotube/particle ratio, 8:2, Figs. 1 and 2). EELS and EDX analyses recorded boron traces at the tips of all long nanotubes (Fig. 3a), implying that boron may have a catalytic effect for the formation of long tubules. Furthermore, ill-formed caps, occasionally open or with negative curvature regions (see Fig. 2), are also observed with B at their ends.

Some of the analysed samples exhibited anomalous graphitic interlayer spacing variations (*ca.* 3.5-3.6Å) within the tubules, greater than in graphite and carbon nanotubes¹⁹. In some cases, these spacing irregularities alternate periodically; for example, a single interlayer spacing at *ca.* 3.5Å, greater than in graphite and typical carbon tubes, appears every five graphitic layers possessing plane-to-plane separations of *ca.* 3.4Å. (see Fig. 4). The latter spacing irregularities could be attributed to defects caused by the generation of non-cylindrical tubules (*eg.* polygonal tubular structures), in which the sharp edges within these polyhedra could generate such spacing irregularities.

It is interesting to note that *most* of the nanotubes contain pure carbon along the main body of the tube and boron traces at their tips. Nevertheless, EELS

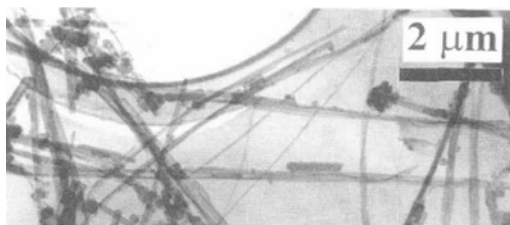


Fig. 1. TEM images showing a representative area where long nanotubes are grown. The amount of polyhedral particles is notably reduced.

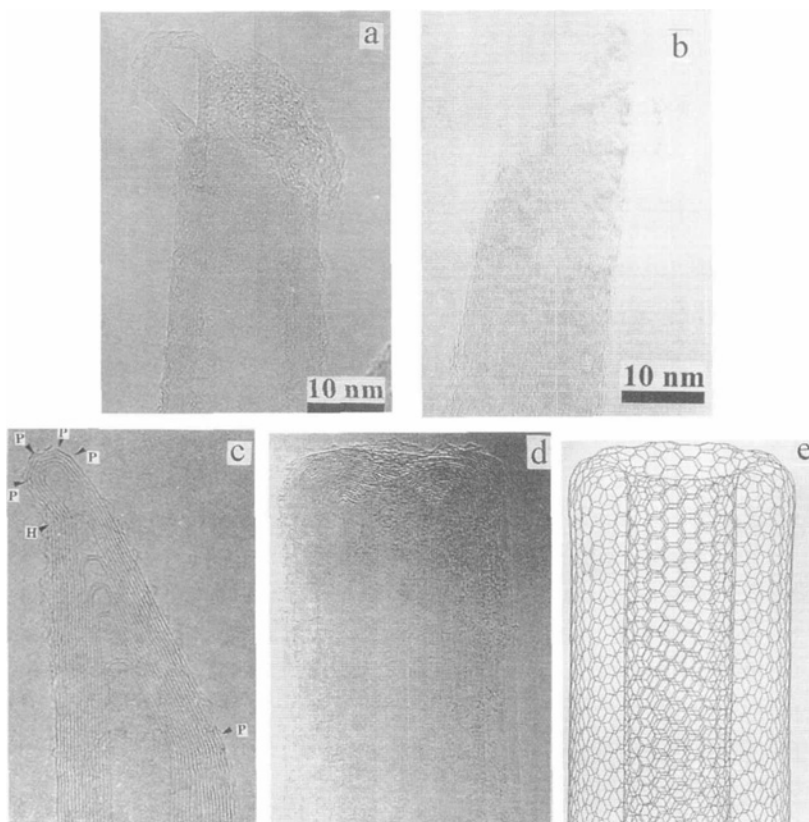


Fig. 2. HRTEM images from: a) III-formed nanotube cap, in which one segment of the tube is closed creating a diamond-like shape and the other end remained open with amorphous material surrounding the tip. b) opened nanotube cap showing amorphous material at the tip. c) Nanotube tip showing negative curvature regions, in which the presence of heptagonal and pentagonal rings may be responsible. P and H denote pentagons and heptagons respectively. d) Hemitoroidal nanotube cap, in which the presence of heptagons and pentagons should also occur. e) Molecular simulation of hemitoroidal nanotube cap containing heptagonal and pentagonal rings along its rim.

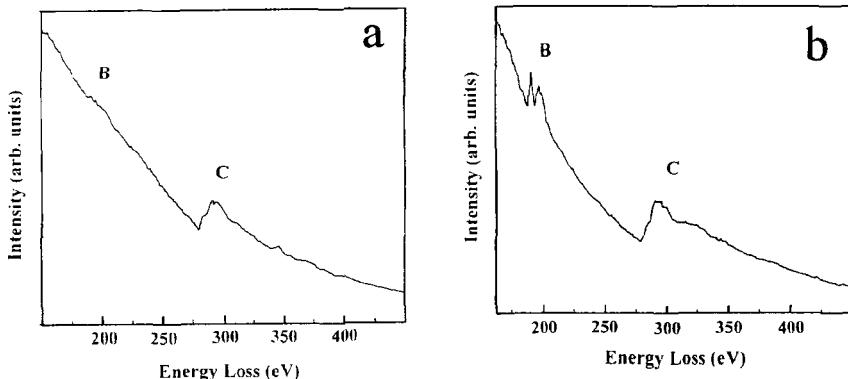


Fig. 3. a) EELS spectra from a typical long tubule tip, which exhibits ionisation edges in the K-shell of boron (*ca.* 188 eV) and carbon (*ca.* 284 eV). The structures of the sharp features observed in carbon indicate sp^2 hybridisation (graphitic arrangements), while the weak intensities from boron suggest small concentrations at the tip. It is noteworthy that no boron was detected within the main body of the generated tubules. This suggest that boron plays a catalytic effect in the production of long graphite nanotubes. b) EELS spectra from a BC_3 nanotube showing sharp ionisation edges at *ca.* 188 eV (suggesting trigonal hybridisation).

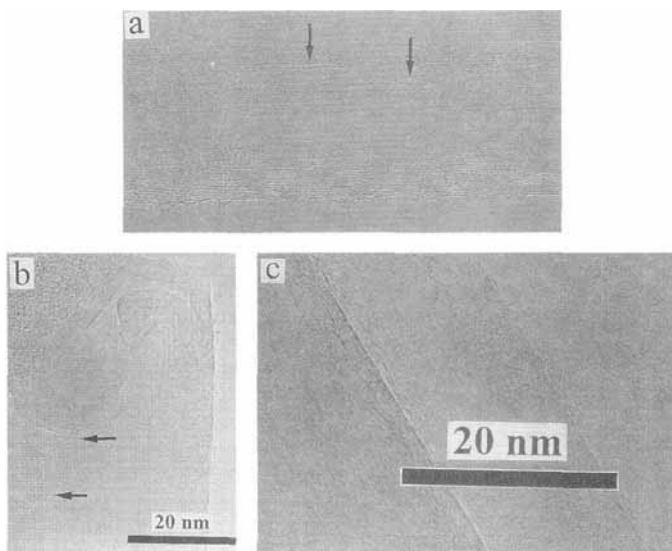


Fig. 4. a) Nanotube segment, in which larger interlayer spacings are observed in one side of the tubule. b) Part of a nanotube tip with interlayer spacing defects every 5-8 layers (denoted by arrows). c) graphite segments formed during B/BN - graphite arc experiments exhibiting interlayer spacings of *ca.* 3.35 Å.

analysis of some nanotubes exhibit ionisation edges at 188 and 284 eV which correspond to the characteristic K-shell ionisation edges of boron and carbon respectively (Fig. 3b). The structure of these sharp features indicates that B and C possess sp^2 hybridisation as in graphite. Stoichiometries of BC_3 within these tubes was estimated from the previous spectra and has been reported elsewhere³⁰.

On the other hand, thick carbon fibres (*ca.* 20 μ m in length and 4 μ m in width) possessing inner cores were also observed. The internal structure of these fibres was difficult to identify (see Fig. 5).

SEM images reveal regions where long nanotubes are agglomerated and surrounded by flake-like structures (possibly B_4C from XRD studies) with an average diameter of 4 μ m. Other regions exhibiting thick fibres with non-straight shapes were also observed (see Fig. 6).

3.2 X-ray patterns from the inner core cathode deposits

From the X-ray powder diffraction pattern (Fig. 7), it is clear that the produced material is more crystalline when compared to normal carbon inner core deposits (carbon nanotubes and/or nanoparticles)¹⁹. This result is due to the presence of crystalline boron carbide (B_4C) crystals and graphite-like structures. A simulation of a B_4C crystal³⁶ was performed (see Fig. 8), finding that the similarity with the *bulk* material produced experimentally is very close. From the (002) reflection (graphite-like structures), two different *average* interlayer spacings arise. These spacings correspond to normal carbon nanotubes/nanoparticles (*ca.* 3.4 Å) and AB graphite (*ca.* 3.35 Å, see Fig. 4c). Estimating the Full Width at Half Maximum (FWHM) for the (002) peaks and using the Bragg equation, it is possible to estimate that the number of layers along the c-axis is consistent with HRTEM observations (*ca.* 40 layers or 20 shells).

It is interesting to point out that the structure of B_4C consists of boron icosahera joint by carbon atoms, exhibiting a rhombohedral structure (space group R-3m) with lattice parameters of: $a = 5.6$ Å, $c = 12.12$ Å. These cage-like boron structures can be generated by arc discharge techniques. Further experiments with boron, exclusively, should be carried out in order to see the possibility of producing larger cages like in fullerenes.

Mass spectrometry studies from the wall chamber soots reveal the presence of higher fullerenes (*e.g.* C_{76} , C_{78} , C_{84} , *etc.*). This is due to the introduction of B and/or BN inside the graphite anode. From Fig. 9 it is clear a larger C_{70}/C_{60} ratio



Fig. 5. HRTEM image from fibres found in the arc using BN-graphite mixtures. It is clear the appearance of inner core.

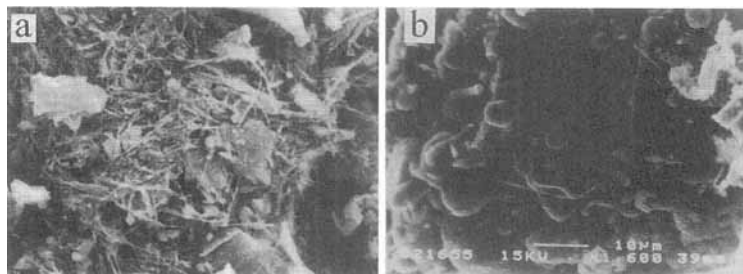


Fig. 6. SEM images from a) the inner core cathode deposits (BN-graphite experiments), in which the presence of long nanotubes ($\leq 16 \mu\text{m}$) is observed as well as flake-like structures with an average diameter of $4 \mu\text{m}$. b) region where non-straight and thick fibres (ca. $20 \mu\text{m}$ in length and $4 \mu\text{m}$ in width) are observed in absence of nanotubes.

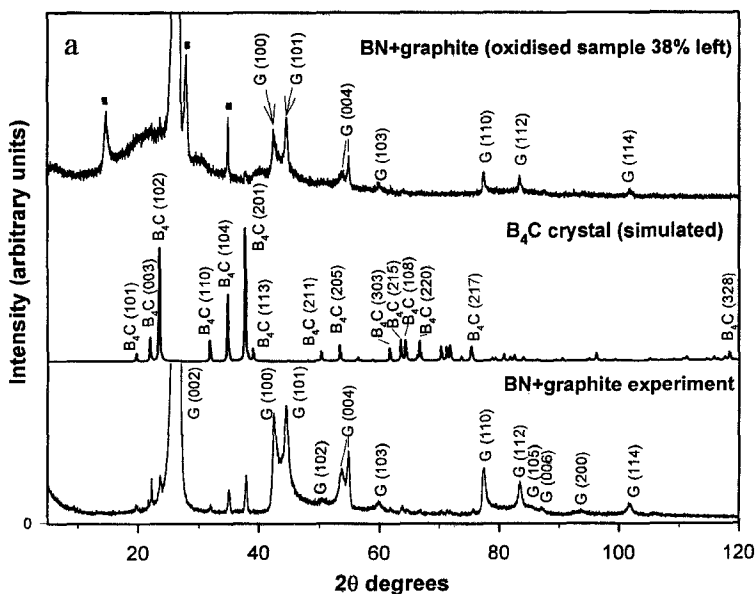


Fig. 7. a) X-ray powder diffraction from the oxidised and non-oxidised inner core cathode deposits. It is clear that the reflections arising from B₄C have disappeared after oxidation and the (00 l) from carbon nanotubes (at *ca.* 3.4 Å) have decreased. However, intensities from (00 l) coming from graphite and/or graphite-like structures have remained (at *ca.* 3.35 Å). The oxidised sample reveals 3 new peaks (square marked boxes), possible due to the production of B₆O.

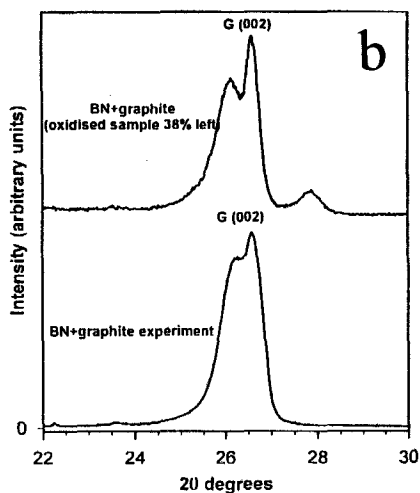


Fig. 7. cont. b) (002) reflections arising from BN-graphite and oxidised inner core deposits. The peak attributed to nanotubes (*ca.* 3.4 Å) has decreased after oxidation, while the one at *ca.* 3.35 Å has remained stable.

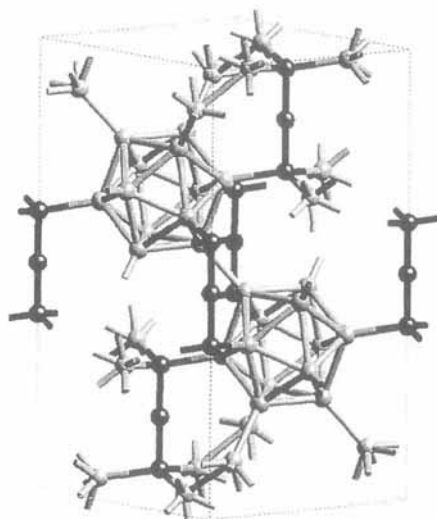


Fig. 8. B_4C crystal lattice exhibiting boron icosahedra joint by carbons. This is a rhombohedral structure belonging to the $R\bar{3}m$ space group and lattice parameters of: $a = 5.6 \text{ \AA}$, $c = 12.12 \text{ \AA}$.

(*ca.* 1:4) when compared to normal graphite plasma arcs (C_{70}/C_{60} ratio at *ca.* 1:10). Therefore, a potential route to higher fullerenes is now available for their bulk production.

When inner core cathode deposits are oxidised ($750 \text{ }^\circ\text{C}$ / oxygen flow at *ca.* 45 ml/min) for 30 and 50 min, *ca.* 38% of the original material is invariably left. X-ray powder diffraction studies from these oxidised deposits exhibit lower intensities from the (002) reflection corresponding to spacings at *ca.* 3.4 \AA . However, intensities from the other (002) reflection, which corresponds to graphite-like material (at *ca.* 3.5 \AA), remains stable (Fig. 7). Additionally, three new peaks appear at high angles, which correspond to a phase of boron oxide (possibly B_6O). HRTEM studies on oxidised deposits show that neither nanotubes nor particles remain, only amorphous-like and curved graphitic material are observed. The nature of the oxidised products are currently under investigation. After oxidation the intensities from B_4C crystals disappear completely. Therefore, it is possible that boron oxide is produced from reactions of B and B_4C with oxygen,

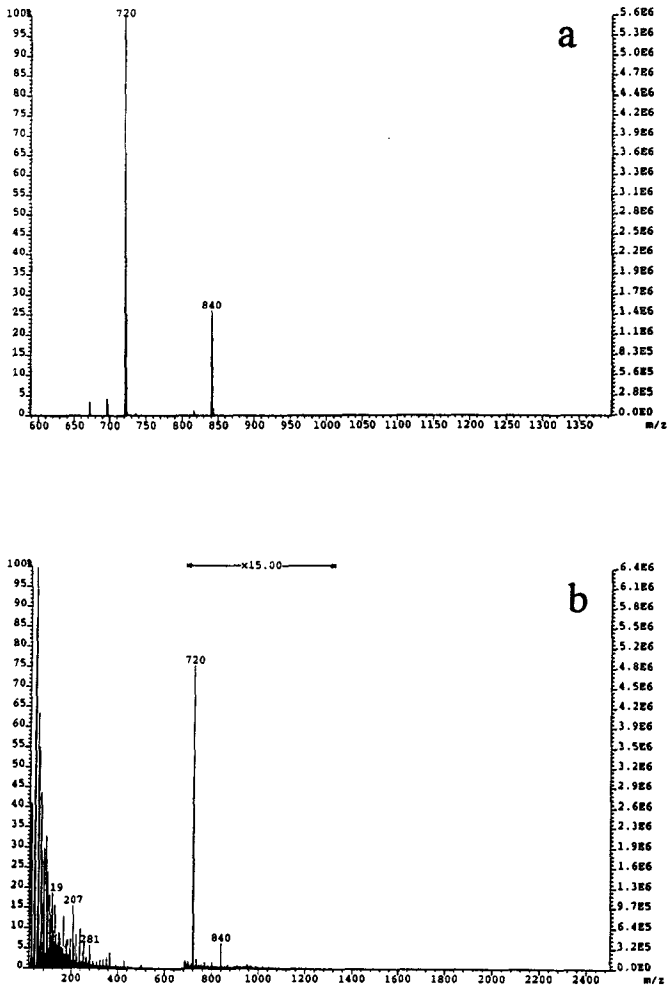


Fig. 9. a) Mass spectra from soot generated by arcing BN/graphite in He atmospheres, showing a $C_{70}:C_{60}$ ratio of *ca.* 1:4. b) Typical mass spectra from soot generated by arcing pure graphite, exhibiting a $C_{70}:C_{60}$ ratio of *ca.* 1:10.

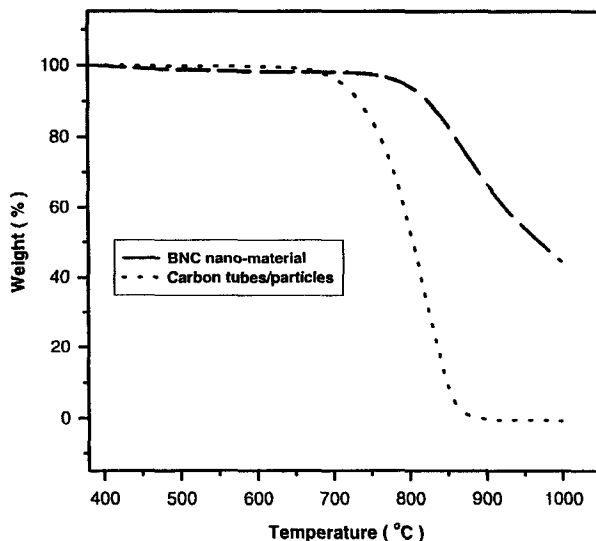


Fig. 10. TGA analysis from BN/C and C deposits, exhibiting that BN/C deposits are stronger to oxidation than pure carbon nanotube/nanoparticles. This may be due to the possible coating of boron oxide which protects some graphite-like domains against oxidation.

generating an oxide coating layer(s), involving graphite-like segments and other nanostructures, thus creating an oxidation resistant material.

Thermogravimetric analyses from different inner core deposits show that BN/graphite cathode deposits never oxidises completely, always *ca.* 40% of the original deposit remains. Nevertheless, typical carbon inner core deposits, containing nanotubes and nanoparticles oxidises completely at 860 °C (see Fig 10).

Experiments inserting B_2O_3 powders inside the graphite anode generates carbon nanotubes without crystalline phases of B_4C . X-ray powder diffraction from these deposits show the production of typical nanotube/particle material (see Fig. 11). Therefore, only B and BN could generate B_4C crystals and BC_3 nanotubes.

CONCLUSIONS

In summary, the effect of B or BN is vital for the production of long graphite nanotubes with B at their tips exhibiting, occasionally, ill-formed caps, in

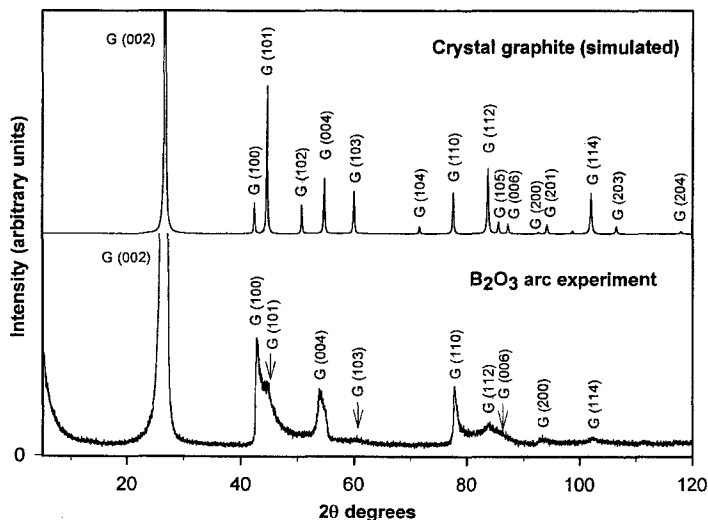


Fig. 11. X-ray powder diffraction from inner core cathode deposits when B_2O_3 is inserted inside the graphite anode. It is clear that B_4C crystals or other boron compounds are not produced. The reflections only arise from normal carbon nanotubes/nanoparticles deposits.

addition to higher yields of larger fullerenes. This may offer tangible applications in nanoengineering due to the high degree of graphitisation and length within the tubes. Furthermore, these material contains phases of B_4C crystals in addition to BC_3 nanotubes, which present interesting structural features responsible for excellent oxidation resistance. It is possible that boron oxide (B_2O_3) is reduced, thus coating graphitic nanostructures which are oxygen stable. Further investigation is currently underway and new horizons in boron chemistry and materials is forthcoming for the next century.

Acknowledgements

We are grateful to Luis Rendón, Julian Thorpe, J. P. Zhang for providing HRTEM facilities and H. W. Kroto, D. R. M. Walton, N. Grobert, J. P. Hare, R. A. García-Cruz and K. Prassides for useful discussions. We thank CONACYT-México (MT, SR, RC and HT), DGAPA UNAM grant IN107-296 (HT) and the ORS scheme for scholarships (MT and WKH).

References

1. Kroto, H. W., Heath, J. R., O'Brien, S. C., Curl, R. F., Smalley, R. E., *Nature* 1985, 318, 162.
2. Krätschmer, W., Lamb, L. D., Fostiropoulos, K., Huffman, D. R., *Nature* 1990, 347, 354.
3. Iijima, S., *Nature* 1991, 354, 56.
4. Ebbesen, T. W. & Ajayan, P. M., *Nature* 1992, 358, 220.
5. Iijima, S., *J. Cryst. Growth* 1980, 5, 675.
6. Ugarte, D. *Nature* 1992, 359, 707.
7. Taylor, R., Langley, G.J., Kroto, H. W., Walton, D. R. M., *Nature* 1993, 366, 728.
8. Crowley, C., Kroto, H. W., Taylor, R., Walton, D. R. M., Bratcher, M.S., Cheng, P. C., and Scott, L. T., *Tetrahedron Lett.* 1995, 36, 9215.
9. Endo, M., Takeuchi, K., Shiraiishi, M., Kroto, H. W., *J. Phys. Chem. Solids* 1993, 54, 1841.
10. Endo, M., Takeuchi, K., Takahashi, K., Kroto, H. W., Sarkar, A., *Carbon* 1995, 33, 873.
11. Howard, J. B., Lafleur, A. L., Markarovsky, Y., Mitra, S., Pope, C. J., Yadav, T. K., *Carbon* 1992, 30, 1183.
12. Guo, T., Nikoleav, P., Rinzler, A. G., Tomélněk, D., Colbert, D. T., Smalley, R. E., *J. Phys. Chem.* 1995, 99, 10694.
13. Thess, A., Lee, R., Nikolaev, P., Dai, H., Petit, P., Robert, J., Xu, C., Lee, Y. H., Kim, S. G., Rinzler, A. G., Colbert, D. T., Scuseria, G. E., Tománek, D., Fischer, J. E., Smalley, R. E., *Science* 1996, 273, 483.
14. Hsu, W.K., Hare, J. P., Terrones, M., Harris, P. F. J., Kroto, H. W. Walton, D. R. M., *Nature* 1995, 377, 687.
15. Hsu, W. K., Terrones, M., Hare, J. P., Terrones, H., Kroto, H. W., Walton, D. R. M., *Chem. Phys. Lett.* 1996, 261, 161.
16. Tsang, S. C., Chen, Y. K., Harris, P. J. F. and Green, M. L. H., *Nature* 1994, 372, 159.
17. McHenry, M. E., Nakamura, Y., Kirkpatrick, S., Johnson, F., Curtin, S., DeGraef, M., Uhfer, N. T., Majetich, S. A., Brunzman, E. M. In *Recent Advances in the Chemistry and Physics of Fullerenes and Related Materials* (ed. K M. Kadish & R. S. Ruoff) 1994, vol. 2, pp. 1463-1475. Electrochemical Society, Pennington, N.J.
18. Murakami, Y., Shibata, T., Okuyama, K., Arai, T., Suematsu, H., Yoshida, Y., *J. Phys. Chem. Solids* 1994, 54, 1861.
19. Terrones, M., Hare, J. P., Hsu, W., Kroto, H. W., Lappas, A., Maser, W. K., Pierik, A. J., Prassides, K., Taylor, R., Walton, D. R. M. In *Recent Advances in the Chemistry and Physics of Fullerenes and Related Materials* (ed. K M. Kadish & R. S. Ruoff) 1995, vol. 2, pp. 599-620 Electrochemical Society, Pennington, N.J.
20. Hare, J.P., Hsu, W.K., Kroto, H. W., Lappas, A., Prassides, K., Terrones, M., and Walton, D. R. M., *Chem. Mater.* 1996, 8, 6.

21. Amelinckx, S., Zhang, X. B., Berbaerts, D., Zhang, X. F., Ivanov, V., Nagy, J. B., *Science* 1994, 265, 635.
22. Terrones, H., Terrones, M., Hsu, W. K., *Chem. Soc. Rev.* 1995, 24, 341.
23. Sarkar, A., Kroto, H. W., Endo, M., *Carbon*, 33, 51.
24. Terrones M., Hsu, W. K., Hare, J. P., Walton, D. R. M., Kroto, H. W. and Terrones, H. *Phil. Trans. Roy. Soc. A* 1995, 354, 2055.
25. Bernaerts, D., Zhang, X. B., Zhang, X. F., Amelinckx, S., Van Tendeloo, G., Van Landuyt, J., Ivanov, V., Nagy, J. B., *Phil. Mag. A* 1995, 71, 605.
26. Mackay, A. L. and Terrones, H., *Nature* 1991, 352, 762.
27. Terrones, H., Fayos, J and Aragón, J. L., *Acta Metallurgica et Materialia* 1994, 42, 2687.
28. Margulis, L., Saltra, G., Tenne, R., Tallanker, M., *Nature* 1993, 365, 113.
29. Tenne, R., Margulis, L., Genut, M., Hodes, G. *Nature* 1992, 360, 444.
30. Wen-Sieh, Z., Cherrey, K., Chopra, N. G., Blase, X., Miyamoto, Y., Rubio, A., Cohen, M. L., Louie, S. G., Zettl, A., Gronsky, R., *Phys. Rev. B* 1995, 51, 11299; Miyamoto, Y., Rubio, A., Cohen, M. L., Louie, S.G., *Phys. Rev. B* 1994, 50, 4976.
31. Terrones, M., Benito, A. M., Manteca-Diego, C., Hsu, W. K., Osmas, O. Y., Hare, J. P., Reid, D. G., Terrones, H., Cheetham, A. K., Prassides, K., Kroto, H. W., Walton, D. R. M., *Chem. Phys. Lett.* 1996, 257, 576.
32. Stephan, O., Ajayan, P. M., Colliex, C., Redlich, Ph., Lambert, J. M., Bernier, P., Lefin, P., *Science* 1994, 266, 1683.
33. Chopra, N.S., Luyken, R. J., Cherrey, K., Crespi, V. H., Cohen, M. L., Louie, S. G., Zettl, A., *Science* 1995, 269, 966.
34. Terrones, M., Hsu, W. K., Terrones, H., Zhang, J. P., Ramos, S., Hare, J. P., Castillo, R., Prassides, K., Cheetham, A. K., Kroto, H. W., Walton, D. R. M., *Chem Phys. Lett.* 1996, 259, 568.
35. Loiseau, A., Willaime, F., Demoncy, N., Hug, G., Pascard, H., *Phys. Rev. Lett.* 1996, 76, 4737.
36. Wyckoff, R. W. G., *Crystal Structures*, vol 2, pp. 138, 1986, R. E. Krieger Publishing Co., Malabar, Florida.

(Received January 6, 1998)